



Cadmium sulphide incorporated reduced Graphene oxide as counter electrode for dye sensitized solar cell

Sandhya Murali*, F. Michael Raj, S.Vigneswari, A.Jeya Rajendran

Advanced Materials Research Laboratory, Department of Chemistry, Loyola College, Chennai, TN, India.

Abstract : Cadmium sulphide incorporated reduced graphene oxide as counter electrode material was synthesized from graphite using modified Hummer's method. Graphene oxide (GO), reduced graphene oxide (rGO), cadmium sulphide (CdS) and cadmium sulphide incorporated reduced graphene oxide (CdS - rGO) were synthesized by wet chemical methods. The synthesized GO was reduced to rGO using hydrazine hydrate as the reducing agent. The synthesized materials were characterized by XRD, FTIR, SEM, EDAX and UV- Visible absorbance spectroscopy. The XRD data confirmed the formation of GO from graphite. The crystallite grain size for all the synthesized materials were calculated from XRD data using Scherrer's formula as 35.1, 6.0, 9.2 and 4.5 nm for GO, r GO, CdS and CdS- rGO respectively. The FTIR spectra of CdS- rGO revealed peaks confirmed the presence of Cd-S bond. The morphology of synthesized samples of GO possessed a layered structure and CdS- rGO had interlaced layer structure. EDAX spectra revealed the presence of carbon and oxygen in GO and the presence of cadmium and sulphur along with carbon and oxygen in CdS- rGO. The UV- Visible spectra showed a red shift when GO was transformed to rGO and CdS-rGO. Dye sensitized solar cells (DSSC) were fabricated using TiO₂ as photoanode, synthesized materials as photocathode, I⁻/I³⁻ as electrolyte and N 719 ruthenium dye as sensitizer. Fabricated DSSC's were subjected to I-V studies. The photoconversion efficiency was calculated and found that CdS- rGO showed maximum efficiency of 7.2%.

Keywords : Graphene oxide, reduced graphene oxide, CdS incorporated rGO, DSSC, photocathode.

Introduction

The development of sustainable and clean energy resources is becoming more promising as the conventional resources are getting depleted. Solar energy utilization, like photovoltaic cells^{1,2}, photocatalysis³ is much sought after as there is an abundant quantity of sunlight that is available all over and also is a process that involve less carbon emission. The invention of the third generation power source also termed as dye sensitized solar cells (DSSC), by Brian'O' Regan and Michael Gratzel, has created a new perspective in the energy conversion process. DSSC's are popular as it is easy to fabricate, is environmental friendly and possess good photoconversion ability⁴. But the production costs of these are high which limit their commercial application. Also, platinum is used as counter electrode(CE) which is quite expensive. The challenge in using

DSSC is to replace the platinum electrode by cheaper material without compromising the efficiency^{5,6}.

Efforts are being made to develop materials from transition metals that could be used as counter electrode that would show high catalytic activity^{7,8,9,10}. Among transition metal compounds, cadmium sulphide has been widely studied due to its smaller band gap(2.4eV) that makes it effective in visible light absorption^{11,12,13}. The synthesis of CdS involves simple process and is a low cost process. However, the efficiency obtained using CdS has found to be very low and also CdS is easily subjected to photo-corrosion. These disadvantages led to the synthesis of material comprising of CdS and material like graphene oxide. Graphite reacts with strong oxidizing agents, such that oxygen containing functionalities are introduced in the graphite structure. The oxidized graphite is called graphite oxide which is a compound made up of carbon, hydrogen and oxygen¹⁴. When graphite oxide is sonicated it exfoliated into one or many layers which is called as graphene oxide (GO). GO is easily dispersible in water and other organic solvents compared to graphite oxide. GO can be differentiated from graphite oxide by its number of layers present in the synthesized material. Many recent research work have been carried out with graphene sheets incorporating into the inorganic metal nanoparticles to enhance its activity. However graphene has been increasingly used as a support for metal or metal oxides with excellent activity¹⁵. The presence of oxygen group in GO sheet helps to attach with the inorganic nanoparticles¹⁶. The controlled reduction of GO forms sp³clusters resulting in the formation of semiconductor material¹⁷.

Research works have been carried out in GO-CdS and rGO-CdS for application in photo catalytic activity and electrochemical studies^{18,19}. Research work based on CdS incorporated rGO towards application in dye sensitized solar cells is not yet reported. So the present work is based on the synthesis of CdS nanoparticles, rGO nanoparticles and CdS- rGO nanocomposites for the application of DSSCs.

Experimental Method

Chemicals and Reagents

All chemicals and reagents such as cadmium acetate dihydrate, (Cd(CH₃COO)₂·2H₂O), graphite (C), sodium sulfide nonahydrate (Na₂S·9H₂O), potassium permanganate (KMnO₄), ortho phosphoric acid (H₃PO₄) and hydrazine hydrate (N₂H₄), were purchased from Avra and Spectrochem chemicals which were of analytical grade and were used directly without any further purification. The glass wares were washed thoroughly and dried in hot air oven before use.

Preparation of reduced graphene oxide(rGO) and CdS- rGO

raphene oxide was synthesised from graphite powder by modified Hummer's method²⁰, which was reduced to rGO using hydrazine hydrate. Incorporation of CdS in rGO was carried out using wet chemical method. The well dispersed solution of rGO was completely transferred into 50 mL of cadmium acetate solution and heated at 80°C with stirring for 4 hrs. To the above solution, 50 mL of sodium sulfide solution was added and reaction was continued for 3 hours. The product was washed and dried.

Fabrication of DSSCs

Solar cell was fabricated as a thin coating on the FTO (Fluorine doped tin oxide) plates by doctoral blade method^{21,22}. The active electrodes were prepared using TiO₂. The coated plates were sintered at 120°C for 2 hours and was dipped in ruthenium dye and sintered at 120°C for four hours. Three counter electrode were prepared using synthesized nanoparticles. Two binder clips were used to hold the electrode together and the liquid electrolyte (I⁻ /I³⁻) were drawn into the space between the electrodes by capillary action.

Instrumentation / characterization

XRD patterns of the synthesized samples were recorded using XPERT PRO analytical instrument (MAC Science MO3XHF22) with a scan rate of 2.0 min⁻¹, an accelerating voltage of 40kV, an applied current of 30mA and using Cu K α radiation. The optical properties were studied in the range of 200-900 nm using **Jasco V-700** UV-Visible spectrophotometer. The Fourier transform infrared spectra (FTIR) were recorded in the range of 450-4500cm⁻¹ using **Schimidzu IR AFFINITY-1S**. The morphology and composition of the sample were studied using the instrument **FEI Quanta 200**, Environmental SEM and **EDX, HITACHI S2400**

respectively. Solar cells were fabricated and the current- voltage measurement were studied by GS610 YOGOKAWA source measurement unit.

Results and Discussion

XRD analysis

XRD analysis was employed to determine the phase, structure and grain size of the particles. Fig 1 shows the XRD pattern of CdS, rGO and CdS-rGO nanocomposites. The XRD pattern of CdS revealed the formation of cubic zinc blende structure exhibiting only three broad peaks at $26.4^\circ(111)$, $43.8^\circ(220)$, $51.8^\circ(311)$ ((ICDD) PDF 41-1049). XRD pattern of rGO revealed the formation of layered sheet like structure which exhibits only one broad peak at $24.59^\circ(002)$ in accordance with the diffraction data (JCPDS file No.41-4019). The reduction of graphene oxide into rGO is also confirmed by the XRD pattern of rGO²³. The complete disappearance of peak at 10° and the formation of peak at 24.59° confirms the presence of rGO.

XRD pattern of the synthesized CdS-rGO exhibited only three broad peaks at $26.5^\circ(002)$, $43.8^\circ(220)$, and $51.9^\circ(311)$ diffraction data ((ICDD) PDF 89-0440). The XRD pattern of CdS-rGO nanocomposite displays all peaks corresponding to CdS and no obvious peak is observed for rGO in the composite. This could be due to the growth of CdS nanoparticles within the graphene interlayers which probably affect the regular stacking leading to exfoliation^{24,25}. The crystallinity of CdS has been retained and the presence of graphene material has not affected CdS²⁶. The crystallite size was calculated using Debye Scherer's formula²⁷, and it was found to be 7.2, 5.3 and 4.5 nm for CdS, rGO and CdS-rGO respectively.

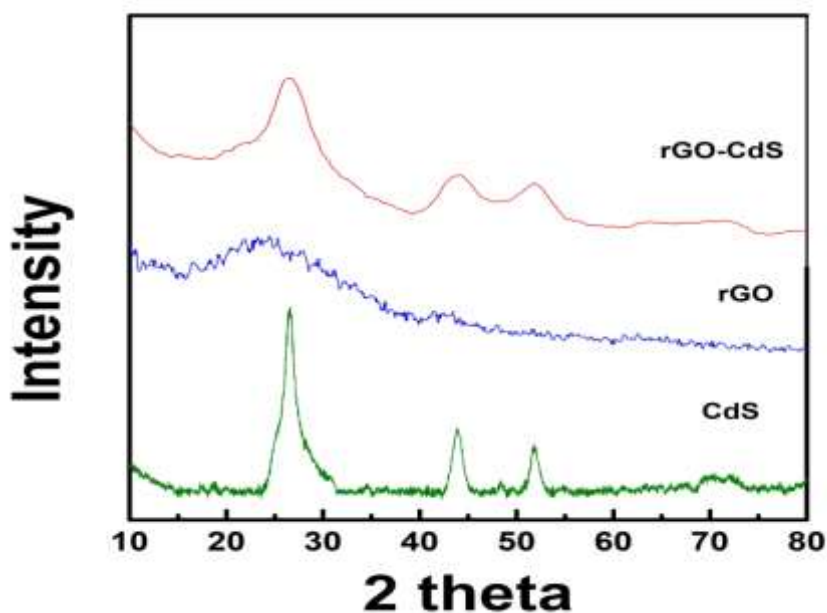


Fig1. XRD pattern for CdS NPs, rGO NPs and CdS-rGO nanocomposites

Table1. Physical characteristics values by XRD analysis

Sample	Peak Position (2θ) $^\circ$	FWHM (β)	Lattice Strain(ϵ) Gpa	Lattice Parameter \AA	Volume (V) (\AA) ³	Average Crystallite Size (D)
CdS	26.4	0.00464	0.00453	5.8	198.2	7.2
rGO	24.5	1.34	0.305	3.38	38.6	5.3
CdS-rGO	26.5	0.75	0.48	a = 4.14 c = 6.71	70.9	4.5

Morphology and Elemental Composition

SEM measurements were carried out for CdS NPs, rGO NPs and CdS-rGO nanocomposites. Fig 2 (a) shows a SEM morphology of CdS NPs which reveals the spherical shape. Fig 2 (b) corresponds to interlaced layer like pattern confirms the presence of reduced graphene oxide. Fig 2 (c) clearly reveals that the distribution of CdS NPs over rGO sheets. CdS-rGO shows sheet like pattern with elevations and depressions inferring that CdS nanoparticles have grown on the surface of rGO. Hence it was confirmed that the CdS NPs have been successfully incorporated into rGO.

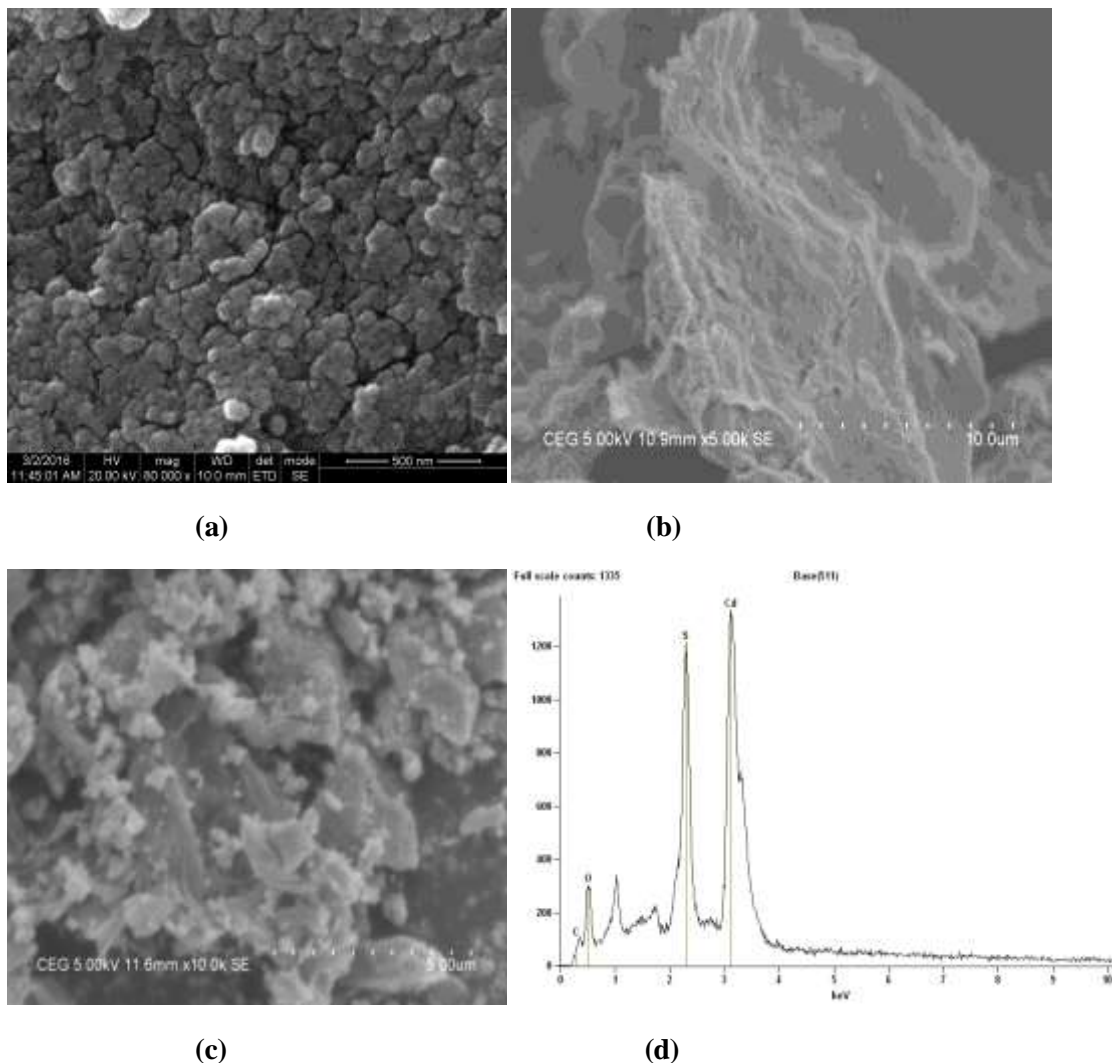


Fig 2. SEM image of (a) CdS NPs (b) rGO NPs and (c) CdS-rGO Nanocomposites and(d) EDAX spectrum of CdS- rGO nanocomposites.

The EDAX spectrum of CdS-rGO nanocomposites [Fig 2(d)] shows the presence of elements with no other impurities. The Table 2 gives the composition of elements present in CdS-rGO nanocomposites.

Table 2 EDAX spectral data for CdS-rGO nanocomposites

Sample	Elemental	Weight percentage (%)
CdS-rGO	C	09.26
	O	42.53
	Cd	28.79
	S	19.42
	Total	100.0

Optical Properties

Fig. 3 shows the UV-visible absorption spectra of synthesized reduced graphene oxide, CdS NPs and CdS-rGO nanocomposites. The rGO nanoparticles has an absorption peak at ~ 262 nm, CdS nanoparticles has absorption peak at ~ 425 nm and the CdS-rGO absorption peak at ~ 315 nm. It is obvious from the UV-Vis absorption spectra that a blue shift of about 110 nm is observed in the absorption edge of CdS nanoparticles on the graphene surface in CdS-rGO composite in comparison to pure CdS nanoparticles. Noteworthy rise in the absorption intensity and hypsochromic shift shows significant improvement in the optical properties of the composite sample in comparison to CdS nanoparticles. This can prove beneficial for enhancing the visible light capturing potential of the synthesized nanocomposite and hence used as counter electrode in solar cells. A significant red shift of about 53 nm is observed in the absorption edge of CdS nanoparticles on the graphene surface in CdS-rGO composite in comparison to pure rGO nanoparticles. The absorption intensity and bathochromic shift shows significant improvement in the optical properties of the composite sample in comparison to rGO nanoparticles. It was deduced that there is strong interaction between rGO and CdS linked on it, which facilitates the nucleation and growth of nanoparticles on the graphene surface

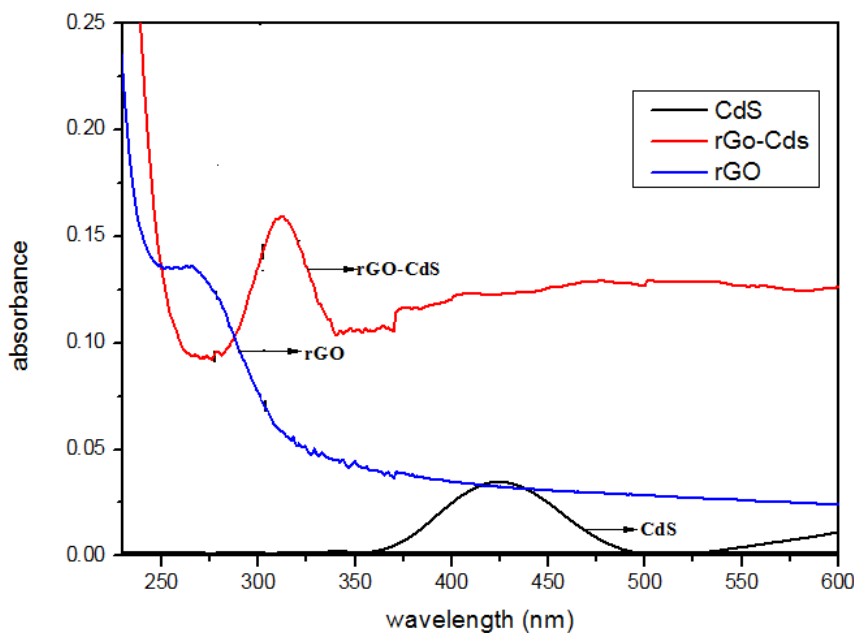


Fig. 3 UV-Vis absorption spectra of CdS NPs, rGO NPs and CdS-rGO nanocomposites

Fourier transform infrared spectroscopy

The spectra of CdS shows (Fig. 4) peak at $3600-3100$ cm^{-1} which could be attributed to the $-\text{OH}$ group of water adsorbed by the samples. Small peak near $400-470$ cm^{-1} indicated the formation of CdS nanoparticles as this region was assigned to metal-sulphur (M-S) bond. The peak at 650 cm^{-1} corresponded to the characteristic peak of CdS. For the rGO, the FTIR results shows that peaks corresponding to epoxy was observed at 1123.8 cm^{-1} , peak due to $-\text{OH}$ was reduced in intensities in the FTIR spectra of rGO. The peak at 2333.29 cm^{-1} may be due to the formation of layered structured of rGO²⁸. Compared with the spectra of GO, there was almost no C-O and O-H absorption bands in CdS-rGO spectra, which meant that majority of the oxygen-containing groups were reduced. For CdS-rGO the FTIR results confirms the presence of CdS and rGO by the peak at $1000-1120$ cm^{-1} which may be due to presence of C-O or S-O (acetone or sulphate) and the sharp peak around 650 cm^{-1} may be due to the presence of the CdS.

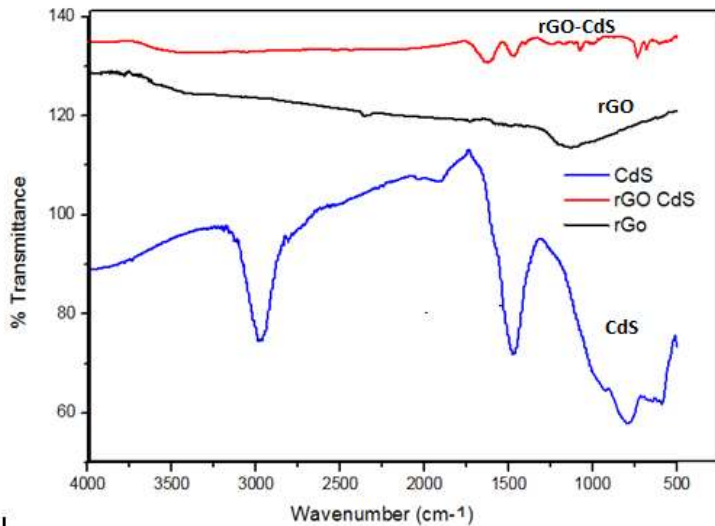


Fig. 4 FTIR spectra of rGO NPs, CdS NPs and CdS-rGO nanocomposites

Photovoltaic studies

The photovoltaic cell was fabricated using titanium dioxide as photoanode, synthesized materials CdS, rGO and CdS-rGO as photocathode (counter electrode), ruthenium N719 dye as sensitizer and I^-/I^{3-} as electrolyte. The fabricated cells were subjected to I-V studies. Fig. 5 gives the photovoltaic parameters and the solar cell efficiency were calculated. The photovoltaic parameters, short circuit current (J_{sc}), open circuit voltage (V_{oc}), fill factor (FF) and power conversion efficiency (η) were calculated from the J-V (Table 3). The average short- circuit current (J_{sc}) for the cells is higher in the DSSC where reduced graphene oxide is the counter electrode. The higher J_{sc} in reduced graphene oxide solar cell is due to its greater light harvesting capacity²⁹. The efficiency of a solar cell is defined as the output power density divided by the input power density. If the incoming light has a power density (P_{in}), the efficiency will be

$$\eta = V_o \times J_{sc} \times FF / P_{in} \text{-----1}$$

The fill factor (FF) is defined as the ratio of the product of the maximum power output (P_m) to the product of short circuit photo current and open circuit voltage

$$FF = I_{mp} \times V_{mp} / V_{oc} \times J_{sc} \text{----- 2}$$

Where I_{mp} and V_{mp} represent the photocurrent and photovoltage corresponding to the maximum power. The four parameters J_{sc} , V_{oc} , FF and η are used to characterize the performance of a solar cell (Table 3).

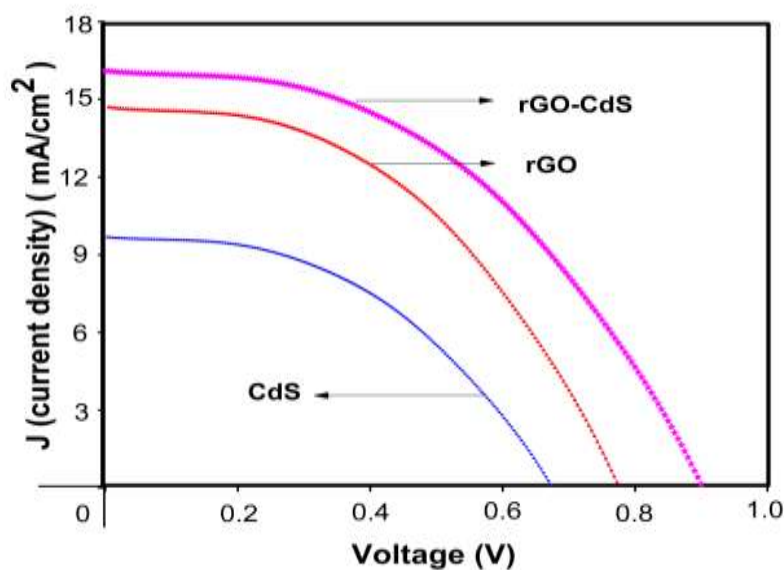


Fig 5. J-V Graph of CdS NPs, rGO NPs and CdS-rGO nanocomposites

Table 3 J-V characteristics data of CdS , rGO and CdS-rGO

Sample	J _{sc} (mA/cm ²)	V _{oc} (V)	FF	η (%)
CdS	9.8	0.68	0.52	2.7
rGO	14.7	0.76	0.58	5.6
CdS-rGO	16.4	0.88	0.68	7.2

Conclusion

Graphene oxide was synthesized by modified Hummer's method and was reduced to rGO using hydrazine hydrate as reducing agent. Cadmium sulphide was incorporated into rGO by wet chemical method.

The structure of synthesized materials were determined by XRD analysis cubic zinc blende, layered sheet for CdS and rGO nanoparticles. The FTIR data of CdS, the presence Cd-S bond was confirmed. The FTIR spectra of rGO shows the absence of absorption peaks corresponding to oxygen functionalities thereby confirming that the reduction process has taken place effectively. The successful incorporation of CdS in rGO was also confirmed by FTIR. The optical properties of synthesized products was also determined. The morphological studies of synthesized compound were carried out and its elemental composition were determined by EDAX. CdS NPs are strong in interaction with rGO nanosheets which is appealing for the photocatalytic applications and their ability to develop unique electron transfer properties. Compared to CdS and rGO nanoparticles, CdS incorporated reduced graphene oxide showed more efficiency of 7.2% in DSSCs.

References

1. Lee C.Y, Van Le Q, Kim C, Kim S.Y. Use of silane-functionalized graphene oxide in organic photovoltaic cells and organic light-emitting diodes. *Phys. Chem. Chem. Phys.* 17,2015, 9369-9374.
2. Lee D.H, Song D, Kang Y.S, Park W.I. Three-Dimensional Monolayer Graphene and TiO₂ Hybrid Architectures for High-Efficiency Electrochemical Photovoltaic Cells. *The J. Phys. Chem. C* 119,2015, 6880-6885.
3. Pan X, Xu Y.J. Graphene-Templated Bottom-up Fabrication of Ultralarge Binary CdS-TiO₂ Nanosheets for Photocatalytic Selective Reduction. *J. Phys. Chem., C* 119,2015, 7184-7194.

- Hagfeldt A, Graetzel M. Light-induced redox reactions in nanocrystalline systems. *Chem. Rev.* 95,1995, 49-68.
- Xin X, He M, Han W, Jung J, Lin Z. Low-cost copper zinc tin sulfide counter electrodes for high-efficiency dye-sensitized solar cells. *Angewandte Chemie International Edition* 50,2011, 11739-11742.
- Yeh M.H, Lin L.Y, Chang L.Y, Leu Y.A, Cheng W.Y, Lin J.J, Ho K.C. Dye-Sensitized Solar Cells with Reduced Graphene Oxide as the Counter Electrode Prepared by a Green Photothermal Reduction Process. *Chem. Phys. Chem.* 15,2014, 1175-1181.
- Zhang J, Najmaei S, Lin H, Lou J. MoS₂ atomic layers with artificial active edge sites as transparent counter electrodes for improved performance of dye-sensitized solar cells. *Nanoscale* 6,2014, 5279-5283.
- Guo S.Q, Jing T.Z, Zhang X, Yang X.B, Yuan Z.H, Hu F.Z. Mesoporous Bi₂S₃ nanorods with graphene-assistance as low-cost counter-electrode materials in dye-sensitized solar cells. *Nanoscale* 6, 2014, 14433-14440.
- Chang S.H, Lu M.D, Tung Y.L, Tuan H.Y. Gram-scale synthesis of catalytic Co₉S₈ nanocrystal ink as a cathode material for spray-deposited, large-area dye-sensitized solar cells. *ACS nano* 7,2013, 9443-9451.
- Patil S.A, Kalode P. Y, Mane R.S, Shinde D.V, Doyoung A, Keumnam C, Han S.H. Highly efficient and stable DSSCs of wet-chemically synthesized MoS₂ counter electrode. *Dalton Transactions* 43,2014, 5256-5259.
- Chen Z, Liu S, Yang M.Q, Xu Y.J. Synthesis of uniform CdS nanospheres/graphene hybrid nanocomposites and their application as visible light photocatalyst for selective reduction of nitro organics in water. *ACS applied materials & interfaces* 5, 2013, 4309-4319.
- Li L.B, Wang Y.F, Rao H.S, Wu W.Q, Li K. N, Su C.Y, Kuang D.B. Hierarchical Macroporous Zn₂SnO₄-ZnO Nanorod Composite Photoelectrodes for Efficient CdS/CdSe Quantum Dot Co-Sensitized Solar Cells. *ACS applied materials & interfaces* 5,2013, 11865-11871.
- Kumar S, Girish K.S, Koteswara Rao. Physics and chemistry of CdTe/CdS thin film heterojunction photovoltaic devices: fundamental and critical aspects. *Energy & Environmental Science* 7,2014, 45-102.
- Humers W. S, Offeman R. E. Preparation of graphitic oxide. *J Am Chem Soc* 80, 1958, 1339.
- Pen, W.T, Wenchao Y, Xiaoyan Li. Synthesis of a sulfur-graphene composite as an enhanced metal-free photocatalyst. *Nano Res.* 6, 2013, 286-292.
- Kaveri S, Thirugnanam L, Dutta M, Ramasamy J, Fukata N. Thiourea assisted one-pot easy synthesis of CdS/rGO composite by the wet chemical method: structural, optical, and photocatalytic properties. *Ceramics International* 39,2013, 9207-9214.
- Shukla S, Saxena S. Spectroscopic investigation of confinement effects on optical properties of graphene oxide. *App. Phys. Lett.* 98, 2011, 073104.
- Zeng P, Zhang Q, Peng T, Zhang X. One-pot synthesis of reduced graphene oxide-cadmium sulfide nanocomposite and its photocatalytic hydrogen production. *Phys. Chem. Chem. Phys.* 13, 2011, 21496-21502.
- Yang H, Kershaw S. V, Wang Y, Gong X, Kalytchu S, Rogach A. L, Teoh W. Y. Shuttling photoelectrochemical electron transport in tricomponent CdS/rGO/TiO₂ nanocomposites. *J. Phys. Chem. C* 117,2013, 20406-20414.
- Marcano D. C, Kosynkin D. V., Berlin J. M, Sinitskii A, Su Z, Slesarev A, Tour, J. M. Improved synthesis of graphene oxide. *Am. Chem. Soc. Nano* 4, 2010, 4806-4816.
- O'regan B, & Grätzel M. A low-cost, high-efficiency solar cell based on dye-sensitized colloidal TiO₂ films. *Nature* 353,1991, 737-740.
- Wang Z. S, Kawauchi H, Kashima, T, Arakawa H. Significant influence of TiO₂ photoelectrode morphology on the energy conversion efficiency of N719 dye-sensitized solar cell. *Coord. chem. rev.* 248, (13), 2004, 1381-1389.
- Krishnamoorthy K, Veerapandian M, Yun K, Kim S. J. The chemical and structural analysis of graphene oxide with different degrees of oxidation. *C* 53, 2013, 38-49.
- Li Q, Guo B, Yu J, Ran J, Zhang B, Yan H, Gong J. R. Highly efficient visible-light-driven photocatalytic hydrogen production of CdS-cluster-decorated graphene nanosheets. *J Am Chem Soc* 133, 2011, 10878-10884.

25. Azarang M, Shuhaimi A, Yousefi R, Sookhakian, M. Effects of graphene oxide concentration on optical properties of ZnO/RGO nanocomposites and their application to photocurrent generation. *J. App. Phys.* 116, 2014, 084307.
26. Zhang J, Yu J, Jaroniec M, Gong J. R. Noble metal-free reduced graphene oxide-Zn_xCd_{1-x}S nanocomposite with enhanced solar photocatalytic H₂-production performance. *Nano lett.* 12, 2012, 4584-4589.
27. Patterson, A.L. The Scherrer formula for X-ray particle size determination. *Phys rev* 56, 1939, 978.
28. Calizo I, Balandin A.A, Bao W, Miao F, Lau C.N. Temperature dependence of the Raman spectra of graphene and graphene multilayers. *Nano lett.* 7(9), 2007, 2645-2649.
29. Guo S Q, Sun M.Q, Gao G D, Liu L. Scalable low-cost CdS nanospheres@ graphene nanocomposites counter electrode for high efficiency dye-sensitized solar cells. *Electrochimica Acta* 176, 2015, 1165-1170.

For your Research References Requirements, always log on to –

www.sphinxesai.com

International Journal of ChemTech Research,

International Journal of PharmTech Research
